

ZU-TH-76/25
November 11, 2025

Probing Lepton Flavour Universality with Λ_b decays to $\tau^+\tau^-$ final states

MARZIA BORDONE,^a GINO ISIDORI,^a
CHRISTIANE MAYER,^a AND JAN-NIKLAS TOELSTEDE^{a,b}

^a*Physik-Institut, Universität Zürich, CH-8057 Zürich, Switzerland*

^b*Paul Scherrer Institut, Forschungsstrasse 111, CH-5232 Villigen, Switzerland*

Abstract

We present a study of the rare baryonic decay $\Lambda_b \rightarrow \Lambda \tau^+ \tau^-$ as a probe of new physics (NP) coupled preferentially to third-generation fermions. Within the Standard Model, we evaluate the branching ratio and the lepton-flavour-universality (LFU) ratio $R_{\Lambda}^{\tau/\mu}$, including both perturbative and long-distance charm contributions. We show that the LFU ratio can be predicted with an uncertainty below 10%. Possible NP effects arising from lepton non-universal dynamics are analysed within an effective field theory framework motivated by the current anomalies in $b \rightarrow c \tau \nu$ and $b \rightarrow s \mu^+ \mu^-$ transitions. In this context, $R_{\Lambda}^{\tau/\mu}$ can be enhanced by several orders of magnitude, offering a clear target for upcoming searches. The implications for the related mode $\Lambda_b \rightarrow p K \tau^+ \tau^-$ are also briefly discussed.

1 Introduction

One of the most interesting and well-motivated hypothesis about the ultraviolet completion of the Standard Model (SM) is that it consists of new degrees of freedom coupled predominantly to third-generation fermions, at least at nearby energy scales. This first layer of New Physics (NP) should also be coupled weakly and in an almost flavour-universal manner to the lighter families. This general setup is supported by the observed fermion mass hierarchies and the electroweak hierarchy problem, while being consistent with the absence of significant deviations in flavour-changing processes and electroweak precision tests [1]. Direct searches at the LHC are also considerably weaker for new states coupled mainly to third-generation fermions, which can still be as light as 1–2 TeV [2].

In order to test this hypothesis via flavour observables, a particularly interesting role is played by the flavour-changing neutral current (FCNC) transitions of the type $b \rightarrow s\tau^+\tau^-$. Experimentally, these modes are extremely challenging to access, and current bounds are still several orders of magnitude above the SM expectations. Nevertheless, the potential NP effects in these channels can be very large: in well-motivated scenarios, the enhancement over SM rates may reach up to three orders of magnitude (see e.g. Ref. [3–7]). Recent improvements in sensitivity from the LHCb [8] and Belle II [9] collaborations have begun to open this window, with future prospects appearing especially promising. Even if the SM regime remains out of reach, the expected progress could soon provide meaningful constraints on NP models that predict large effects in these modes.

From a phenomenological point of view, the study of $b \rightarrow s\tau^+\tau^-$ transitions is further motivated by the persistent discrepancies between data and SM predictions observed in both $b \rightarrow s\mu^+\mu^-$ and $b \rightarrow c\tau\nu$ transitions. In the latter case, a clear correlation between charged- and neutral-current processes is dictated by the electroweak symmetry. As a result of this correlation, the Lepton Flavour Universality (LFU) ratios R_D and R_{D^*} imply large enhancements in the $b \rightarrow s\tau^+\tau^-$ rates, if interpreted as a NP signals [3–7]. Moreover, the $b \rightarrow s\tau^+\tau^-$ amplitude thus predicted radiatively induce a smaller deviation in $b \rightarrow s\ell^+\ell^-$ ($\ell = e, \mu$) [10–12] whose magnitude and size is in the right ballpark to explain current tensions in various $b \rightarrow s\mu^+\mu^-$ observables.

In this work, we focus on a specific exclusive $b \rightarrow s\tau^+\tau^-$ process that appears particularly promising for experimental investigation at hadron colliders: the baryonic decay $\Lambda_b \rightarrow \Lambda\tau^+\tau^-$. Baryonic final states offer several experimental advantages, including reduced backgrounds and distinctive kinematic signatures. As we will show, the LFU ratio between the tauonic and muonic modes, $R_\Lambda^{\tau/\mu}$, provides a theoretically clean observable with small hadronic uncertainties. We present the SM prediction for this observable, explore possible NP modifications, and discuss correlations with the current anomalies in $b \rightarrow c\tau\nu$ and $b \rightarrow s\mu^+\mu^-$ transitions. We also discuss how our conclusions can be easily be adopted to the related decay mode $\Lambda_b \rightarrow pK\tau^+\tau^-$.

This paper is organized as follows. In Section 2 we analyse the SM prediction for the $\Lambda_b \rightarrow \Lambda\tau^+\tau^-$ and the LFU ratio $R_\Lambda^{\tau/\mu}$ taking into account both perturbative contributions and long-distance effects related to the narrow charmonium resonances. As a cross-check of our description of the SM amplitude, we also briefly compare our prediction for the dilepton

spectrum in the muon case ($\Lambda_b \rightarrow \Lambda \mu^+ \mu^-$) with current data. In Section 3 we present a general expression for $R_\Lambda^{\tau/\mu}$ in presence of NP and discuss the enhancement expected in view of current anomalies. The results are summarised in the Conclusions.

2 Standard Model predictions

The effective Hamiltonian describing $b \rightarrow s \ell^+ \ell^-$ transitions below the electroweak scale, both within the SM and in the general class of NP models we are interested in, reads

$$\mathcal{H}_{\text{eff}} = -\frac{4G_F}{\sqrt{2}} V_{tb} V_{ts}^* \frac{\alpha_{\text{em}}}{4\pi} \left[\sum_{i=1}^8 C_i(\mu) \mathcal{O}_i(\mu) + \sum_{i=9,10} C_i^\ell \mathcal{O}_i^\ell(\mu) \right], \quad (2.1)$$

where

$$\begin{aligned} \mathcal{O}_1 &= (\bar{s}_L^\alpha \gamma_\mu c_L^\beta)(\bar{c}_L^\beta \gamma^\mu b_L^\alpha), & \mathcal{O}_2 &= (\bar{s}_L \gamma_\mu c_L)(\bar{c}_L \gamma^\mu b_L), \\ \mathcal{O}_9^\ell &= (\bar{s}_L \gamma_\mu b_L)(\bar{\ell} \gamma^\mu \ell), & \mathcal{O}_{10}^\ell &= (\bar{s}_L \gamma_\mu b_L)(\bar{\ell} \gamma^\mu \gamma^5 \ell), \\ \mathcal{O}_7 &= \frac{m_b}{e} (\bar{s}_R \sigma_{\mu\nu} b_L) F^{\mu\nu}. \end{aligned} \quad (2.2)$$

The remaining operators, \mathcal{O}_{3-8} , with suppressed Wilson coefficients and vanishing tree-level matrix elements, can be found e.g. in Ref. [13]. Within the SM, lepton flavour universality implies

$$C_{9(10)}^e|_{\text{SM}} = C_{9(10)}^\mu|_{\text{SM}} = C_{9(10)}^\tau|_{\text{SM}}. \quad (2.3)$$

We thus omit to indicate the lepton superscript in the Wilson coefficients C_9^ℓ and C_{10}^ℓ in the rest of this section. We will put it back in Section 3 when discussing non-universal NP effects.

Predicting observables for $\Lambda_b \rightarrow \Lambda \ell^+ \ell^-$ decays involves evaluating hadronic matrix elements of the type $\langle \Lambda(p_\Lambda) | \mathcal{O}_i | \Lambda_b(p_{\Lambda_b}) \rangle$. We can distinguish three cases:

- The contribution from local semileptonic $\mathcal{O}_{7,9,10}$ operators. These effects are encoded in hadronic local form-factors, scalar functions that depend on the momentum transfer $q^2 = (p_{\Lambda_b} - p_\Lambda)^2$. To describe the $\Lambda_b \rightarrow \Lambda \ell^+ \ell^-$ decays, we need ten independent form factors. For the purposes of this analysis, we use the definitions in App. A and the numerical results from Lattice QCD computations in [14].
- The contribution from the four-quark operators \mathcal{O}_{1-6} . Due to Lorentz and gauge invariance, the contributions from these operators to the decay amplitude can be easily introduced as a q^2 dependent shift to C_9 , defined as

$$C_9 \rightarrow C_9^{\text{eff}} = C_9 + Y(q^2). \quad (2.4)$$

For simplicity, we can further decompose $Y(q^2)$ depending on the quark flavour:

$$Y(q^2) = Y_{q\bar{q}}(q^2) + Y_{c\bar{c}}(q^2) + Y_{b\bar{b}}(q^2), \quad (2.5)$$

where the first term accounts for light quarks contribution, and the last two for charm and bottom quark contributions, respectively. At leading order in α_s , the function $Y(q^2)$ can be calculated perturbatively. It reads

$$\begin{aligned} Y_{q\bar{q}}^{(0)}(q^2) &= \frac{4}{3}C_3 + \frac{64}{9}C_5 + \frac{64}{27}C_6 - \frac{1}{2}h(q^2, 0) \left(C_3 + \frac{4}{3}C_4 + 16C_5 + \frac{64}{3}C_6 \right), \\ Y_{c\bar{c}}^{(0)}(q^2) &= h(q^2, m_c) \left(\frac{4}{3}C_1 + C_2 + 6C_3 + 60C_5 \right), \\ Y_{b\bar{b}}^{(0)}(q^2) &= -\frac{1}{2}h(q^2, m_b) \left(7C_3 + \frac{4}{3}C_4 + 76C_5 + \frac{64}{3}C_6 \right), \end{aligned} \quad (2.6)$$

with

$$h(q^2, m) = -\frac{4}{9} \left(\ln \frac{m^2}{\mu^2} - \frac{2}{3} - x \right) - \frac{4}{9}(2+x) \begin{cases} \sqrt{x-1} \arctan \frac{1}{\sqrt{x-1}}, & x = \frac{4m^2}{q^2} > 1, \\ \sqrt{1-x} \left(\ln \frac{1+\sqrt{1-x}}{\sqrt{x}} - \frac{i\pi}{2} \right), & x = \frac{4m^2}{q^2} \leq 1. \end{cases} \quad (2.7)$$

Non-factorisable corrections arising at higher orders in QCD have been calculated in the literature [15,16]. Out of them, we retain only the correction to C_7 as in [17], while we neglect further corrections to C_9 given that they are numerically less important and beyond the sought for precision of this analysis.

- Long-distance effects from $c\bar{c}$ resonances. These are the contributions from the charmonia resonances, that are not described in the previous category. We treat them using dispersive analysis following the approach in [17]. Further details are in the next section.

With this, we have all necessary information to describe the $\Lambda_b \rightarrow \Lambda \ell^+ \ell^-$ decay width. We implement the differential decay width, in terms of Wilson Coefficients and hadronic local form factors, as in App. A. The results therein have been partially crosschecked against [18–20].

2.1 Long-distance $c\bar{c}$ contributions

To include the effects from long-distance charm rescattering contributions, we closely follow the approach of [17], where narrow charmonium resonances are described in terms of a subtracted dispersion relation. However, with respect to [17], we do not distinguish among the possible Λ polarisation due to a lack of experimental information on the relative size of the contribution of each polarisation to the decay rate. In the dispersive approach, we have that the $c\bar{c}$ contribution to C_9^{eff} can be rewritten as

$$Y_{c\bar{c}}(q^2) = -\frac{4}{9} \left[\frac{4}{3}C_1(\mu) + C_2(\mu) \right] \left[1 + \ln \left(\frac{m_c^2}{\mu^2} \right) \right] + \frac{16\pi^2}{\mathcal{F}(q^2)} \sum_V \eta_V e^{i\delta_V} \frac{q^2}{m_V^2} A_V^{\text{res}}(q^2), \quad (2.8)$$

C_1	-0.291 ± 0.009	m_{Λ_b}	5.620 GeV	m_τ	1.776 GeV
C_2	1.010 ± 0.001	m_Λ	1.116 GeV	m_μ	0.106 GeV
C_7^{eff}	-0.450 ± 0.050	m_b	4.87 GeV	m_e	0.511×10^{-3} GeV
C_9	4.273 ± 0.251	$ V_{tb}V_{ts}^* $	0.04185	τ_{Λ_b}	2.2303×10^{12} GeV $^{-1}$
C_{10}	-4.166 ± 0.033	α_{em}	1/133	G_F	1.166×10^{-5} GeV $^{-2}$

Table 1: Inputs used in the numerical analysis. The Wilson Coefficients, $C_i(\mu)$, evaluated at $\mu = m_b$, are from Ref. [17].

where the first term is the subtraction term at $q^2 = 0$, and each resonance V is parametrised as Breit-Wigner

$$A_V^{\text{res}}(q^2) = \frac{m_V \Gamma_V}{m_V^2 - q^2 - im_V \Gamma_V}, \quad (2.9)$$

with $V = J/\psi, \psi(2S)$, and we neglected the subleading terms proportional to parametrically small Wilson coefficients. In this context, \mathcal{F} is an appropriate combination of local form factors that, for the $\Lambda_b \rightarrow \Lambda \ell^+ \ell^-$ case, reads

$$\mathcal{F}^2(q^2) = \frac{m_{\Lambda_b}^2}{\lambda(m_{\Lambda_b}^2, m_\Lambda^2, q^2)} \kappa_{99}(q^2), \quad (2.10)$$

where

$$\kappa_{99}(q^2) = \frac{4}{3} \left[2(|f_\perp|^2 s_- + |g_\perp|^2 s_+) + \frac{(m_{\Lambda_b} + m_\Lambda)^2}{q^2} |f_+|^2 s_- + \frac{(m_{\Lambda_b} - m_\Lambda)^2}{q^2} |g_+|^2 s_+ \right], \quad (2.11)$$

with $f_{\perp, \pm}$ and $g_{\perp, \pm}$ defined in App. A and $s_\pm = (m_{\Lambda_b} \pm m_\Lambda)^2 - q^2$. The function $\kappa_{99}(q^2)$ is nothing but the combination of hadronic form factors appearing in the $|C_9|^2$ term in differential rate (see App. A). With the \mathcal{F} thus defined, we can extract η_V for each resonance from data. Given the definition in (2.8), the branching ratio for the resonance-mediated process $\Lambda_b \rightarrow \Lambda V \rightarrow \Lambda \ell^+ \ell^-$ is

$$\begin{aligned} \mathcal{B}(\Lambda_b \rightarrow \Lambda V \rightarrow \Lambda \ell^+ \ell^-) &= (16\pi^2)^2 \mathcal{B}^{(0)} |\eta_V|^2 \int_{4m_\ell^2}^{(m_{\Lambda_b} - m_\Lambda)^2} dq^2 |A_V^{\text{res}}(q^2)|^2 \times \\ &\quad \times \kappa_{99}(q^2) \sqrt{\lambda_H(q^2) \lambda_L(q^2)} \left(1 + \frac{2m_\ell^2}{q^2} \right) \frac{1}{|\mathcal{F}(q^2)|^2} \left(\frac{q^2}{m_V^2} \right)^2 \\ &= \frac{(16\pi^2)^2 |\eta_V|^2 \mathcal{B}^{(0)}}{m_{\Lambda_b}^2} \int_{4m_\ell^2}^{(m_{\Lambda_b} - m_\Lambda)^2} dq^2 \lambda_H^{3/2}(q^2) \lambda_L^{1/2}(q^2) \frac{q^2(q^2 + 2m_\ell^2)}{m_V^4} |A_V^{\text{res}}(q^2)|^2, \quad (2.12) \end{aligned}$$

where we have defined

$$\lambda_H(q^2) = \lambda(m_{\Lambda_b}^2, m_\Lambda^2, q^2), \quad \lambda_L(q^2) = \lambda(q^2, m_\ell^2, m_\ell^2), \quad \mathcal{B}^{(0)} = \frac{G_F^2 \alpha_{\text{em}}^2 |V_{tb}V_{ts}^*|^2 \tau_{\Lambda_b}}{2048\pi^5 m_{\Lambda_b}^3}, \quad (2.13)$$

V	m_V	Γ_V	$\mathcal{B}(\Lambda_b \rightarrow V\Lambda)$	$\mathcal{B}(V \rightarrow e^+e^-)$
$J/\psi(1S)$	3.097 GeV	92.6×10^{-6} GeV	$(3.34 \pm 0.31) \times 10^{-4}$	$(5.971 \pm 0.032) \times 10^{-2}$
$\psi(2S)$	3.686 GeV	293.0×10^{-6} GeV	$(1.70 \pm 0.18) \times 10^{-4}$	$(7.94 \pm 0.22) \times 10^{-3}$

Table 2: Masses and decay widths of the narrow charmonium states J/ψ and $\psi(2S)$. All values are taken from [22], except $\mathcal{B}(\Lambda_b \rightarrow V\Lambda)$, for which we use only the latest LHCb measurement [21]. See text for more details.

with $\lambda(a, b, d) = a^2 + b^2 + c^2 - 2ab - 2bc - 2ac$. In the narrow-width approximation, which is well motivated for $V = J/\psi, \psi(2S)$, we find

$$|\eta_V|^2 = \frac{m_{\Lambda_b}^2}{2^{8\pi^5} m_V \Gamma_V} \times \frac{\mathcal{B}(\Lambda_b \rightarrow \Lambda V) \mathcal{B}(V \rightarrow \Lambda \ell^+ \ell^-)}{\mathcal{B}^{(0)} \lambda_H^{3/2} (m_V^2) \lambda_L^{1/2} (m_V^2) (1 + 2m_\ell^2/m_V^2)}. \quad (2.14)$$

where we use the factorisation $\mathcal{B}(\Lambda_b \rightarrow \Lambda V \rightarrow \Lambda \ell^+ \ell^-) = \mathcal{B}(\Lambda_b \rightarrow \Lambda V) \mathcal{B}(V \rightarrow \Lambda \ell^+ \ell^-)$, as expected in the narrow-width approximation. Note that the m_ℓ dependence in the denominator of (2.14) cancels the one in $\mathcal{B}(V \rightarrow \ell^+ \ell^-)$. As a result, in the narrow-width approximation η_V is independent of the lepton mass.

The relevant parameters needed to obtain the values of the η_V values from (2.14) are in Table 2. For the production of the J/ψ resonance, we use the latest measurement of the LHCb collaboration [21], and we reconstruct the production of the $\psi(2S)$ resonance from this measurement and the world average of the ratio

$$\frac{\Gamma(\Lambda_b \rightarrow \psi(2S)\Lambda)}{\Gamma(\Lambda_b \rightarrow J/\psi(1S)\Lambda)} = 0.508 \pm 0.023. \quad (2.15)$$

in [22]. Using the values for the parameters in Tables 1-2, we obtain: $\eta_{J/\psi(1S)} = 38.0 \pm 1.8$ and $\eta_{\psi(2S)} = 6.65 \pm 0.36$. Concerning the phases, there are no measurements that can be employed to constrain them. Therefore, if not stated otherwise, in the following numerical analysis, we always consider them to have a flat distribution between 0 and 2π .

2.2 Predictions for branching ratios and LFU ratios

With the previous parametrisation of the resonances, we can now compute observables for the $\Lambda_b \rightarrow \Lambda \tau^+ \tau^-$ decay. We start by studying the di-lepton branching fraction. Our prediction is depicted in Fig. 1, where the blue band encodes the 1σ region accounting for the uncertainties from the local form factors and the resonance parameters. As can be seen, above $q^2 \gtrsim 14 \text{ GeV}^2$ the large effect coming from the $\psi(2S)$ resonance, which cannot be precisely controlled, is suppressed.

In Table 3 we present results for the integrated $\mathcal{B}(\Lambda_b \rightarrow \Lambda \tau^+ \tau^-)$ in the region $q^2 > 15 \text{ GeV}^2$. In order to provide a reliable estimate, in Table 3 we study the impact associated with various sources of uncertainty. In the first three rows we set $\delta_{J/\psi} = \delta_{\psi(2S)} = 0$, and investigate the size of the relative uncertainties coming from the local form-factors and the

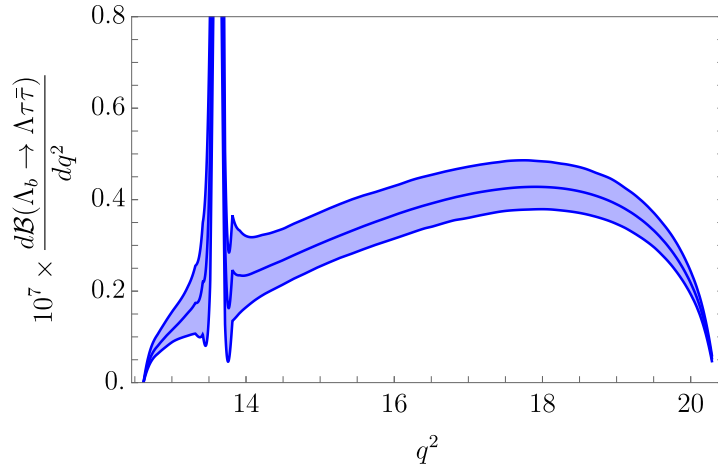


Figure 1: Predictions of the differential branching ratio of $\Lambda_b \rightarrow \Lambda\tau^+\tau^-$ as a function of the di-lepton invariant mass q^2 in GeV^2 . The band is the 1σ uncertainty region due to uncertainties from local form factors and resonance parameters. The latter includes varying the phases with a flat distribution within the interval $[0, 2\pi]$.

sources of uncertainty	$10^7 \times \mathcal{B}_{q^2 > 15 \text{ GeV}^2}(\Lambda_b \rightarrow \Lambda\tau^+\tau^-)$
FFs	$1.832^{+0.285}_{-0.218}$
$\eta_{J/\psi}, \eta_{\psi(2S)}$	$1.832^{+0.003}_{-0.003}$
FFs, $\eta_{J/\psi}, \eta_{\psi(2S)}$	$1.832^{+0.285}_{-0.219}$
FFs, $\eta_{J/\psi}, \eta_{\psi(2S)}, \delta_{J/\psi}, \delta_{\psi(2S)}$	$1.933^{+0.295}_{-0.228}$
$\delta_{J/\psi}, \delta_{\psi(2S)}$	$1.933^{+0.059}_{-0.057}$

Table 3: Uncertainties on the integrated branching ratios depending on the sources of uncertainties being considered.

parameters $\eta_{J/\psi}$ and $\eta_{\psi(2S)}$. The uncertainty stemming from the local form factors only is in the first line, and it roughly amounts to about 14%. In the second line, we fix the local form factor parameters to their central values and vary only $\eta_{J/\psi}$ and $\eta_{\psi(2S)}$. Their impact on the uncertainty is found to be subdominant, as confirmed in the third line when we vary them together with the local form factor parameters. In the fourth line, we also vary the phases $\delta_{J/\psi}$, and $\delta_{\psi(2S)}$, assuming a flat distribution for them. We notice that the central value of the branching ratio shifts, due to the fact that various choices for the phases can make the two terms in Eq. (2.8) interfere constructively or destructively. This shift accounts for all possible combinations of phases. Finally, for completeness, in the last line we study the effect of the phase variation while setting all other parameters to their central values. We see that, in the chosen q^2 region, there is a residual $\sim 3\%$ error stemming from the phase variation. Taking this into account, and in the spirit of being conservative, we

assume as nominal prediction:

$$\mathcal{B}(\Lambda_b \rightarrow \Lambda \tau^+ \tau^-) = 1.93^{+0.30}_{-0.23} \times 10^{-7} \quad \text{for} \quad q^2 \geq 15 \text{ GeV}^2. \quad (2.16)$$

We now discuss the LFU ratio $R_\Lambda^{\tau/\mu}$, defined as

$$R_\Lambda^{\tau/\mu} = \frac{\int_{q_{\min}^2}^{(m_{\Lambda_b} - m_\Lambda)^2} \frac{d\mathcal{B}}{dq^2}(\Lambda_b \rightarrow \Lambda \tau^+ \tau^-)}{\int_{q_{\min}^2}^{(m_{\Lambda_b} - m_\Lambda)^2} \frac{d\mathcal{B}}{dq^2}(\Lambda_b \rightarrow \Lambda \mu^+ \mu^-)}. \quad (2.17)$$

Following closely the above discussion, we obtain

$$(R_\Lambda^{\tau/\mu})_{[15 \text{ GeV}^2]}^{\text{SM}} = 0.526 \pm 0.033. \quad (2.18)$$

The relative uncertainty in $R_\Lambda^{\tau/\mu}$ is about 7%, significantly smaller than that of the integrated branching fraction. This is not surprising, given most of the hadronic uncertainties cancel in the ratio between the $\Lambda_b \rightarrow \Lambda \tau^+ \tau^-$ and $\Lambda_b \rightarrow \Lambda \mu^+ \mu^-$ modes. However, differently from the LFU ratios between the muon and electron channels, where a relative precision around 1% is achieved [23], $R_\Lambda^{\tau/\mu}$ has a larger uncertainty due to mass effects that are not negligible when comparing the $\tau^+ \tau^-$ final state with the light leptons case.

To a larger extent, the value of $R_\Lambda^{\tau/\mu}$ is determined by the available phase space, at fixed q_{\min}^2 , and is largely insensitive to the form factor shape. As we shall discuss in the next section, the SM prediction for $R_\Lambda^{\tau/\mu}$ is also mildly sensitive to the value of q_{\min}^2 , provided $q_{\min}^2 \in [15, 17] \text{ GeV}^2$, as it can be seen from the right panel of Table 4. For this reason, the result in Eq. (2.18) is expected to be a reasonable estimate of analog LFU ratios in a similar kinematical range. A particularly interesting mode from the experimental point of view is the $\Lambda_b \rightarrow pK\ell^+\ell^-$ decay, which is dominated by the $\Lambda(1520)$ intermediate state. Using the results for the $\Lambda_b \rightarrow \Lambda(1520)$ local form factors in [24] and the EOS software [25, 26], we estimate

$$(R_{pK}^{\tau/\mu})_{[15 \text{ GeV}^2]}^{\text{SM}} = 0.44 \pm 0.03, \quad (2.19)$$

where the central value has been obtained using only the $\Lambda(1520)$ intermediate state, and the uncertainty is a naïve estimate taking into account the contribution associated with additional intermediate states.

Finally, we further validate our approach by comparing binned predictions for $\mathcal{B}(\Lambda_b \rightarrow \Lambda \mu^+ \mu^-)$ with the latest LHCb measurement [27]. In this work, what is actually measured is the ratio:

$$\frac{\mathcal{B}(\Lambda_b \rightarrow \Lambda \mu^+ \mu^-)|_{q_{\min}^2}^{q_{\max}^2}}{\mathcal{B}(\Lambda_b \rightarrow \Lambda J/\psi)} \quad (2.20)$$

where $q_{\min(\max)}^2$ is the lower(upper) extrema that define the bin length. This implies that obtaining $(\Lambda_b \rightarrow \Lambda \mu^+ \mu^-)|_{q_{\min}^2}^{q_{\max}^2}$ requires an external measurement of $\mathcal{B}(\Lambda_b \rightarrow \Lambda J/\psi)$. In [27], a then up-to-date world average combination was used. However, since then, new measurements of $\mathcal{B}(\Lambda_b \rightarrow \Lambda J/\psi)$ appeared, and, as already discussed in [29], they largely

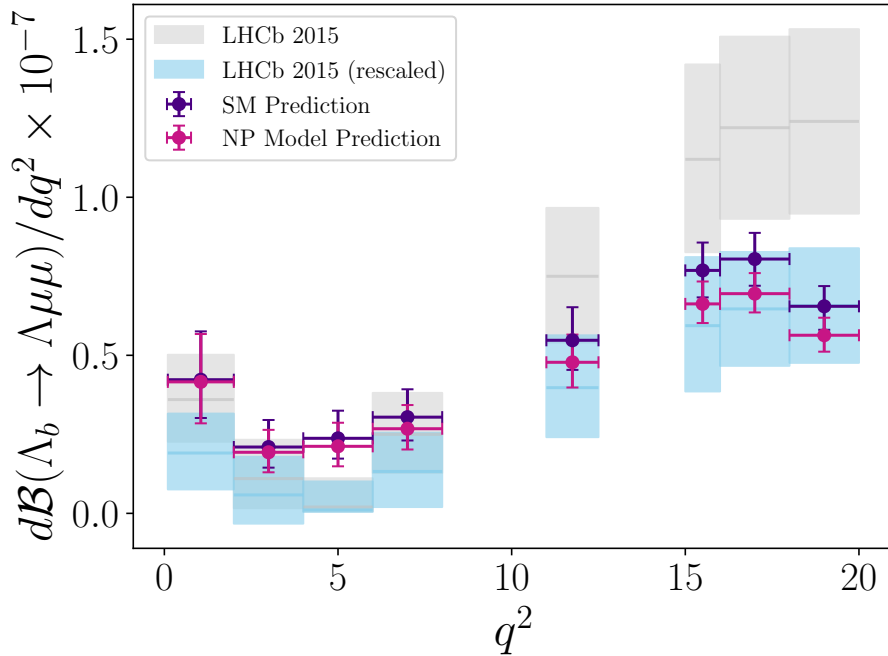


Figure 2: Dilepton spectrum of the $\Lambda_b \rightarrow \Lambda \mu^+ \mu^-$ decay measured by LHCb. The gray areas are the original results reported in [27], while the blue ones are those obtained rescaling the normalization using the recent result for $\mathcal{B}(\Lambda_b \rightarrow \Lambda J/\psi)$ in [28]. The crosses denote our theory prediction in the SM case (violet) and with the NP shift to C_9 discussed in Section 3.2 (purple).

shift the reported values in [27]. We choose to rescale the results in [27] with the latest measurement from LHCb [28], that, at the current status, is the most precise one compared to the world average [22]. The result thus obtained is shown in Fig. 2. Here, in gray we report the values for the rate originally quoted in [27], while in light blue we plot the results of the rescaling just described. To this, we superpose our binned predictions, both in the SM case and in presence of the small NP contribution expected in the muon channel (see Section 3.2). The good agreement between our predictions and the rescaled experimental data provides an important validation of the theoretical description of the hadronic part of the amplitude.

3 Violations of LFU beyond the SM

3.1 General parameterization of NP effects in $R_\Lambda^{\tau/\mu}$

The NP models that we are interested in lead to modifications of the Wilson Coefficients C_9^ℓ and C_{10}^ℓ that, in general, are lepton non-universal. We can parameterize these effects as

$$C_9^\ell = C_9^{\text{SM}} + \Delta C_9^\ell, \quad C_{10}^\ell = C_{10}^{\text{SM}} + \Delta C_{10}^\ell, \quad (3.1)$$

R_{SM}	a_9	b_9	q_{\min}^2	R_{SM}
0.526(33)	0.0460(31)	6.88(22)	15 GeV^2	0.526 ± 0.033
1	-0.92	0.13	16 GeV^2	0.545 ± 0.029
-0.92	1	-0.51	17 GeV^2	0.561 ± 0.024
0.13	-0.51	1	$4m_{\tau}^2$	0.463 ± 0.038

Table 4: Numerical coefficients to evaluate $R_{\Lambda}^{\tau/\mu}$ within and beyond the SM via Eq. (3.2). **Left:** full set of coefficients for $q_{\min}^2 = 15 \text{ GeV}^2$, with correlation matrix. **Right:** SM values for different choices of q_{\min}^2 (for $q_{\min}^2 = 4m_{\tau}^2$ a cut of $\pm 0.1 \text{ GeV}^2$ around $q^2 = m_{\psi(2S)}^2$ is applied).

such that the SM limit is recovered for $\Delta C_9^{\ell} = \Delta C_{10}^{\ell} = 0$. The LFU ratio in Eq. (2.17) is an excellent probe of NP scenarios where $\Delta C_i^{\tau} \neq \Delta C_i^{\mu}$. In principle, within the SM, a tiny breaking of LFU is induced by QED corrections [23]. However, these effects do not exceed a few % and are safely negligible for our purposes. The NP scenarios we are aiming to investigate are those where $|\Delta C_9^{\tau}| \gg |C_9^{\text{SM}}|$ and/or $|\Delta C_{10}^{\tau}| \gg |C_{10}^{\text{SM}}|$, leading to large enhancements of the $\tau^+\tau^-$ modes. In such limit we can also safely neglect $\Delta C_{9(10)}^{\mu}$ in the evaluation of $R_{\Lambda}^{\tau/\mu}$, given the existing constraints on $C_{9,10}^{\mu}$ from $b \rightarrow s\mu^+\mu^-$ transitions.

In the limit $\Delta C_{9,10}^{\mu} = 0$, the prediction for the LFU ratio in Eq. (2.17) can be expressed using ΔC_9^{τ} and ΔC_{10}^{τ} in the form

$$R_{\Lambda}^{\tau/\mu} = R_{\text{SM}} \left[a_9 \left(\frac{b_9}{2} + \Delta C_9^{\tau} \right)^2 + a_{10} \left(\frac{b_{10}}{2} + \Delta C_{10}^{\tau} \right)^2 \right], \quad (3.2)$$

where R_{SM} is the SM value. By construction, the numerical coefficients a_i and b_i satisfy the normalization condition

$$\frac{a_9 b_9^2}{4} + \frac{a_{10} b_{10}^2}{4} = 1. \quad (3.3)$$

Moreover, since the operator \mathcal{O}_{10} does not interfere with the contributions from any other operator, $b_{10} = 2C_{10}$. As a result, taking into account also the normalization condition, the expression (3.2) contains three free parameters, whose numerical values for $q_{\min}^2 = 15 \text{ GeV}^2$ are given in Table 4.

3.2 EFT analysis

As already mentioned in the introduction, possible large NP effects in $b \rightarrow s\tau^+\tau^-$ transitions are motivated by the persistent discrepancies between data and SM predictions observed in both $b \rightarrow s\mu^+\mu^-$ and $b \rightarrow c\tau\nu$ transitions. In this section, we present a correlated analysis of all these effects adopting and extending the EFT framework developed in [30]. The main hypothesis is that at some high scale $\Lambda \sim \text{few TeV}$, the leading NP effects are

encoded in third-generation semi-leptonic operators, with minimal breaking of the $U(2)^5$ flavour symmetry responsible for heavy-light mixing in the left-handed quark sector.

According to the analysis of Ref. [30], scalar operators are strongly constrained by data. This allows us to restrict the attention to the following current-current operators

$$\mathcal{L}_{\text{eff}}^{\text{NP}} \supset C_{\ell q}^+ Q_{\ell q}^+ + C_{\ell q}^- Q_{\ell q}^- + C_{qe} Q_{qe}, \quad (3.4)$$

where

$$\begin{aligned} Q_{\ell q}^\pm &= (\bar{q}_L^3 \gamma^\mu q_L^3) (\bar{\ell}_L^3 \gamma_\mu \ell_L^3) \pm (\bar{q}_L^3 \gamma^\mu \sigma^a q_L^3) (\bar{\ell}_L^3 \gamma_\mu \sigma^a \ell_L^3), \\ Q_{qe} &= (\bar{q}_L^3 \gamma^\mu q_L^3) (\bar{\tau}_R \gamma_\mu \tau_R), \end{aligned} \quad (3.5)$$

and $\ell_L^3 = (\nu_\tau, \tau_L)^T$. The impact of the $U(2)^5$ breaking in the quark sector is taken into account setting

$$q_L^3 = q_L^b - \epsilon V_{ts} q_L^s + O(V_{td} q_L^d), \quad (3.6)$$

where $q_L^{b,s,d}$ are down-aligned doublets. The EFT framework is then described by four independent parameters: $C_{\ell q}^\pm$, C_{qe} , and ϵ . The operator C_{qe} has not been included in Ref. [30] but is worth to consider it in our analysis since it allows us to decouple NP effects in ΔC_9^τ and ΔC_{10}^τ .

Using $\mathcal{L}_{\text{eff}}^{\text{NP}}$ in (3.4) the tree-level values of ΔC_9^τ and ΔC_{10}^τ reads

$$\Delta C_9^\tau = -\epsilon (C_{qe} + 2C_{\ell q}^+) \frac{\pi v^2}{\alpha_{\text{em}}}, \quad \Delta C_{10}^\tau = -\epsilon (C_{qe} - 2C_{\ell q}^+) \frac{\pi v^2}{\alpha_{\text{em}}}, \quad (3.7)$$

where $v = (\sqrt{2}G_F)^{-1/2} \approx 246$ GeV and we have set $V_{tb} = 1$. The operators $Q_{\ell q}^\pm$ also induce a universal shift, relative to the SM, in R_D and R_{D^*} , namely the τ/ℓ ($\ell = e, \mu$) universality ratios of $B \rightarrow D^{(*)}\ell\nu$ transitions. The tree-level result is

$$\frac{R_{D^{(*)}}}{R_{D^{(*)}}^{\text{SM}}} \approx 1 - v^2(1 + \epsilon) (C_{\ell q}^+ - C_{\ell q}^-) = 1 - v^2 r \epsilon C_{\ell q}^+, \quad (3.8)$$

where we defined

$$r = \frac{1 + \epsilon}{\epsilon} \left(1 - \frac{C_{\ell q}^-}{C_{\ell q}^+} \right). \quad (3.9)$$

The global fit of all available data performed in [30] setting $C_{qe} = 0$, including electroweak observables and Drell-Yan processes at the LHC, indicates $\epsilon \approx 3$ and $|C_{\ell q}^-|/|C_{\ell q}^+| \lesssim 0.2$. What is particularly relevant to our analysis is that the sizable value of ϵ and the smallness of $|C_{\ell q}^-|/|C_{\ell q}^+|$ lead to a precise determination of the parameter r in Eq. (3.9): $r = 1.60 \pm 0.15$. As a result, in the absence of right-handed currents, the NP contributions to ΔC_9^τ , ΔC_{10}^τ , and $R_{D^{(*)}}$ are all proportional to $\epsilon C_{\ell q}^+$ and highly correlated. This correlation is exploited in Fig. 3 (left), where we plot the expectation of $R_\Lambda^{\tau/\mu}$ vs. $R_{D^{(*)}}$, both normalised to their corresponding SM values, setting $C_{qe} = 0$. As can be seen, the current anomaly in $R_{D^{(*)}}$ favors huge values $R_\Lambda^{\tau/\mu}$, as high as 5×10^2 or even above.

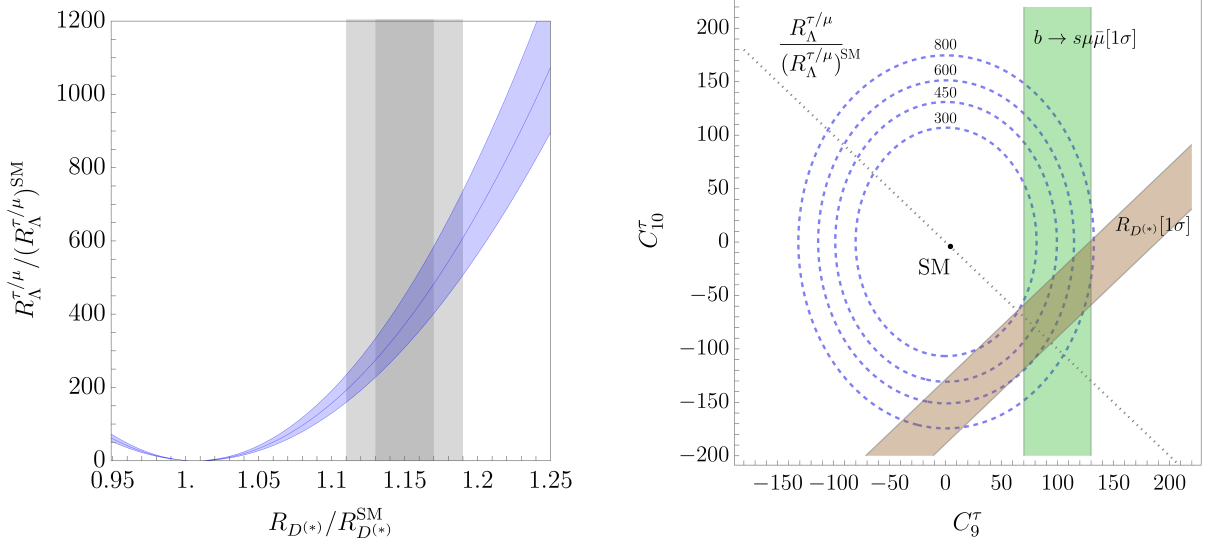


Figure 3: Predictions of $R_A^{\tau/\mu}$ in extensions of the SM with NP predominantly coupled to third-generation fermions. **Left:** correlation $R_A^{\tau/\mu}$ vs. $R_{D^{(*)}}$ in the absence of right-handed currents (blue band); both LFU ratios are normalised to their SM value; the dark (light) gray region indicates the experimental value of $R_{D^{(*)}}$ at 68% CL (98% CL). **Right:** contours in the C_9^τ – C_{10}^τ plane corresponding to different values of $R_A^{\tau/\mu}$ normalised to the SM (dashed circles); the brown and green areas are those currently favored at 68% CL by $b \rightarrow s \mu \bar{\mu}$ and $R_{D^{(*)}}$, respectively; the dotted line indicates the relation $C_9^\tau = -C_{10}^\tau$ expected for left-handed interactions.

Combining constraints from $b \rightarrow s \mu^+ \mu^-$ and $b \rightarrow c \tau \nu$. An independent consistency check of this NP framework is obtained by considering also information derived from $b \rightarrow s \mu^+ \mu^-$ transitions. As pointed out in [11], a huge value of C_9^τ induces, at one-loop level, a non-negligible shift in $C_9^{\mu,e}$. This effect can be estimated unambiguously, as it depends only on the ultraviolet scale Λ at which the NP Lagrangian in Eq. (3.4) is defined. The one-loop calculation yields

$$\Delta C_9^{\mu,e} = -\Delta C_9^\tau \frac{\alpha_{\text{em}}}{6\pi} \log(\Lambda^2/m_\tau^2). \quad (3.10)$$

Current data on $B \rightarrow K^{(*)} \mu^+ \mu^-$ transitions [31–33] indicate a suppression of $C_9^{\mu,e}$ with respect to its SM prediction [12, 17]. A precise estimate of this effect is hampered by possible non-factorizable long-distance contributions. Taking into account the analysis of charm rescattering presented in [34, 35], we estimate $(\Delta C_9^\mu)^{\text{bs}\mu\mu} = -0.6 \pm 0.2$. The impact of this NP contribution in the $\Lambda_b \rightarrow \Lambda \mu^+ \mu^-$ mode is shown in Fig. 2. Using this reference value and inverting Eq. (3.10) we obtain an indication of the preferred value of ΔC_9^τ from $b \rightarrow s \mu^+ \mu^-$ data. The result thus obtained, setting $\Lambda = 1$ TeV is shown by the green band in Fig. 3 (right).

In the same plot we also display the C_9^τ – C_{10}^τ region favoured by $R_{D^{(*)}}$, obtained by

inverting Eq. (3.8) and expressing $\epsilon C_{\ell q}^+$ as

$$\epsilon C_{\ell q}^+ = \frac{\alpha_{\text{em}}}{4\pi v^2} (\Delta C_{10}^\tau - \Delta C_9^\tau) . \quad (3.11)$$

Not surprisingly, the two regions intersect in a parameter space compatible with the relation $C_{10}^\tau = -C_9^\tau$, which holds in the absence of right-handed currents. As also illustrated in Fig. 3 (right), a future measurement of $R_\Lambda^{\tau/\mu}$ would provide a third, independent constraint on the C_9^τ – C_{10}^τ plane and could serve as a decisive test of this NP framework.

4 Conclusion

We have presented a detailed analysis of the rare baryonic decay $\Lambda_b \rightarrow \Lambda\tau^+\tau^-$, focusing on its potential to probe new physics coupled preferentially to third-generation fermions. Using lattice QCD results for the $\Lambda_b \rightarrow \Lambda$ local form factors and employing a dispersive treatment of long-distance charm contributions, we have presented an up-to-date SM prediction for $\mathcal{B}(\Lambda_b \rightarrow \Lambda\tau^+\tau^-)$. As expected, this rate is very suppressed, in the 10^{-7} range, well below the current experimental sensitivity. Most importantly, we have shown that the LFU ratio $R_\Lambda^{\tau/\mu}$ can be predicted very precisely in the SM, with an uncertainty below 10%. This observable can therefore serve as a theoretically clean benchmark to test LFU in baryonic $b \rightarrow s\ell^+\ell^-$ transitions.

Going beyond the SM, we have investigated how much $R_\Lambda^{\tau/\mu}$ can be enhanced in motivated NP scenarios in which new dynamics couple predominantly to third-generation fermions. We have explored the phenomenology of this class of models via a general EFT approach, relating possible lepton non-universal contributions in $b \rightarrow s\tau^+\tau^-$, $b \rightarrow c\tau\nu$, and $b \rightarrow s\mu^+\mu^-$ decay amplitudes. As already noted in the literature, effective NP operators with dominant left-handed currents addressing the $R_{D^{(*)}}$ anomaly naturally imply large enhancements of $b \rightarrow s\tau^+\tau^-$ rates. Interestingly, this scenario also implies a small suppression of the effective coefficient C_9^μ extracted from $b \rightarrow s\mu^+\mu^-$ transitions, an effect which is well consistent with current data. As we have shown, the non-trivial correlations among $R_\Lambda^{\tau/\mu}$, $R_{D^{(*)}}$, and C_9^μ , which could be explored with future data, would provide a clear test of this NP hypothesis.

From an experimental point of view, the $\Lambda_b \rightarrow \Lambda\tau^+\tau^-$ decay enhanced by two orders of magnitude or more, as expected in this class of NP models, is challenging but possibly within the reach of the LHCb experiment in the near future. Our analysis demonstrates that, even in the absence of a direct observation, upper bounds below 10^{-4} would already provide useful constraints on motivated models. The framework we have presented can also be extended to related baryonic channels, in particular to the $\Lambda_b \rightarrow pK\tau^+\tau^-$ decay, which is particularly promising from the experimental point of view. The key aspect is measuring, or setting constraints, on τ/μ LFU ratios, which are largely insensitive to hadronic uncertainties. To this purpose, we have presented the SM value for the τ/μ ratio in $\Lambda_b \rightarrow pK\ell^+\ell^-$.

In summary, rare baryonic decays with $\tau^+\tau^-$ final states offer a powerful and largely unexplored probe of possible new dynamics involving third-generation fermions. The results

presented here, which include precise SM predictions and a model-independent parametrization of possible new-physics effects, offer valuable tools to fully exploit the discovery potential of future measurements.

Acknowledgements

We thank Méril Reboud for helping us obtain **EOS** predictions. We also thank Lesya Shchutska for useful discussions that motivated us to start this work. This research was supported by the Swiss National Science Foundation, projects No. PCEFP2-194272 and 2000-1-240011.

A Differential Branching Ratio

We parametrise the hadronic matrix elements for $\Lambda_b(p, s_{\Lambda_b}) \rightarrow \Lambda(k, s_{\Lambda})$ decays using an helicity decomposition [14, 18, 36, 37]. For the vector and the axial vector current, we have

$$\begin{aligned} \langle \Lambda(k, s_{\Lambda}) | \bar{s} \gamma^{\mu} b | \Lambda_b(p, s_{\Lambda_b}) \rangle = & + \bar{u}_{\Lambda}(k, s_{\Lambda}) \left[f_0(q^2) (m_{\Lambda_b} - m_{\Lambda}) \frac{q^{\mu}}{q^2} \right. \\ & + f_+(q^2) \frac{m_{\Lambda_b} + m_{\Lambda}}{s_+} \left(p^{\mu} + k^{\mu} - (m_{\Lambda_b}^2 - m_{\Lambda}^2) \frac{q^{\mu}}{q^2} \right) \\ & \left. + f_{\perp}(q^2) \left(\gamma^{\mu} - \frac{2m_{\Lambda}}{s_+} p^{\mu} - \frac{2m_{\Lambda_b}}{s_+} k^{\mu} \right) \right] u_{\Lambda_b}(p, s_{\Lambda_b}), \end{aligned} \quad (\text{A.1})$$

$$\begin{aligned} \langle \Lambda(k, s_{\Lambda}) | \bar{s} \gamma^{\mu} \gamma_5 b | \Lambda_b(p, s_{\Lambda_b}) \rangle = & - \bar{u}_{\Lambda}(k, s_{\Lambda}) \gamma_5 \left[g_0(q^2) (m_{\Lambda_b} + m_{\Lambda}) \frac{q^{\mu}}{q^2} \right. \\ & + g_+(q^2) \frac{m_{\Lambda_b} - m_{\Lambda}}{s_-} \left(p^{\mu} + k^{\mu} - (m_{\Lambda_b}^2 - m_{\Lambda}^2) \frac{q^{\mu}}{q^2} \right) \\ & \left. + g_{\perp}(q^2) \left(\gamma^{\mu} + \frac{2m_{\Lambda}}{s_-} p^{\mu} - \frac{2m_{\Lambda_b}}{s_-} k^{\mu} \right) \right] u_{\Lambda_b}(p, s_{\Lambda_b}), \end{aligned} \quad (\text{A.2})$$

while for the tensor and pseudo tensor current we use:

$$\begin{aligned} \langle \Lambda(p', s') | \bar{s} i\sigma^{\mu\nu} q_{\nu} b | \Lambda_b(p, s) \rangle = & - \bar{u}_{\Lambda}(p', s') \left[h_+(q^2) \frac{q^2}{s_+} \left(p^{\mu} + p'^{\mu} - (m_{\Lambda_b}^2 - m_{\Lambda}^2) \frac{q^{\mu}}{q^2} \right) \right. \\ & \left. + h_{\perp}(q^2) (m_{\Lambda_b} + m_{\Lambda}) \left(\gamma^{\mu} - \frac{2m_{\Lambda}}{s_+} p^{\mu} - \frac{2m_{\Lambda_b}}{s_+} p'^{\mu} \right) \right] u_{\Lambda_b}(p, s), \end{aligned} \quad (\text{A.3})$$

$$\begin{aligned} \langle \Lambda(p', s') | \bar{s} i\sigma^{\mu\nu} q_{\nu} \gamma_5 b | \Lambda_b(p, s) \rangle = & - \bar{u}_{\Lambda}(p', s') \gamma_5 \left[\tilde{h}_+(q^2) \frac{q^2}{s_-} \left(p^{\mu} + p'^{\mu} - (m_{\Lambda_b}^2 - m_{\Lambda}^2) \frac{q^{\mu}}{q^2} \right) \right. \\ & \left. + \tilde{h}_{\perp}(q^2) (m_{\Lambda_b} - m_{\Lambda}) \left(\gamma^{\mu} + \frac{2m_{\Lambda}}{s_-} p^{\mu} - \frac{2m_{\Lambda_b}}{s_-} p'^{\mu} \right) \right] u_{\Lambda_b}(p, s), \end{aligned} \quad (\text{A.4})$$

with $q = p - k$, $s_{\pm} = (m_{\Lambda_b} \pm m_{\Lambda})^2 - q^2$, and s_{Λ_b} and s_{Λ} are the spin of the Λ_b and Λ baryons, respectively. With these definitions, we write down the differential branching fraction:

$$\frac{d\mathcal{B}(\Lambda_b \rightarrow \Lambda \ell^+ \ell^-)}{dq^2 d \cos \theta} = \mathcal{B}^{(0)} \frac{\sqrt{\lambda_H(q^2) \lambda_L(q^2)}}{q^2} [A(q^2) + B(q^2) \cos \theta + C(q^2) \cos^2 \theta], \quad (\text{A.5})$$

with $\lambda_{H,L}(q^2)$ and $\mathcal{B}^{(0)}$ defined as in Eq. (2.13) and where the angular coefficients are

$$\begin{aligned} A(q^2) = & |C_{10}|^2 \frac{4m_{\ell}^2}{q^2} \left(M_-^2 s_+ |f_0|^2 + M_+^2 s_- |g_0|^2 \right) \\ & + \left(|C_9|^2 (4m_{\ell}^2 + q^2) - |C_{10}^2| q_+ \right) \left(s_- |f_{\perp}|^2 + s_+ |g_{\perp}|^2 \right) \\ & + \left(|C_9|^2 - \frac{q_+}{q^2} |C_{10}|^2 \right) \left(s_- M_+^2 |f_+|^2 + s_+ M_-^2 |g_+|^2 \right) \\ & + |C_7|^2 \frac{4m_b^2}{q^4} \left(s_- (q^4 |h_+|^2 + M_+^2 (q^2 + 4m_{\ell}^2) |h_{\perp}|^2) + s_+ (q^4 |\tilde{h}_+|^2 + M_-^2 (q^2 + 4m_{\ell}^2) |\tilde{h}_{\perp}|^2) \right) \\ & + \frac{4m_b}{q^2} \left(M_+ s_- (q^2 \Re(C_7 C_9^* h_+ f_+^*) + (q^2 + 4m_{\ell}^2) \Re(C_7 C_9^* h_{\perp} f_{\perp}^*)) \right. \\ & \left. + M_- s_+ (q^2 \Re(C_7 C_9^* \tilde{h}_+ g_+^*) + (q^2 + 4m_{\ell}^2) \Re(C_7 C_9^* \tilde{h}_{\perp} g_{\perp}^*)) \right), \end{aligned} \quad (\text{A.6})$$

$$B(q^2) = -\sqrt{-\frac{q_+ \lambda_H}{q^2}} \left(8m_b \left(M_- \Re(C_7 C_{10}^* \tilde{h}_{\perp} f_{\perp}^*) + M_+ \Re(C_7 C_{10}^* h_{\perp} g_{\perp}^*) \right) + 8q^2 \Re(C_9 C_{10}^*) \Re(f_{\perp} g_{\perp}^*) \right), \quad (\text{A.7})$$

$$\begin{aligned} C(q^2) = & (|C_9|^2 + |C_{10}|^2) \frac{q_+}{q^2} \left(s_- (M_+^2 |f_+|^2 - q^2 |f_{\perp}|^2) + s_+ (M_-^2 |g_+|^2 - q^2 |g_{\perp}|^2) \right) \\ & + |C_7|^2 \frac{4m_b^2 q_+}{q^4} \left(s_- (q^2 |h_+|^2 - M_+^2 |h_{\perp}|^2) + s_+ (q^2 |\tilde{h}_+|^2 - M_-^2 |\tilde{h}_{\perp}|^2) \right) \\ & + 4m_b \frac{q_+}{q^2} \left(M_+ s_- \Re(C_7 C_9^* (h_+ f_+^* - h_{\perp} f_{\perp}^*)) + M_- s_+ \Re(C_7 C_9^* (\tilde{h}_+ g_+^* - \tilde{h}_{\perp} g_{\perp}^*)) \right), \end{aligned} \quad (\text{A.8})$$

where we define $q_+ = 4m_{\ell}^2 - q^2$ and $M_{\pm} = (m_{\Lambda_b} \pm m_{\Lambda})$.

References

[1] J. Davighi and G. Isidori, *Non-universal gauge interactions addressing the inescapable link between Higgs and flavour*, *JHEP* **07** (2023) 147 [2303.01520].

- [2] L. Allwicher, C. Cornella, G. Isidori and B. A. Stefanek, *New physics in the third generation. A comprehensive SMEFT analysis and future prospects*, *JHEP* **03** (2024) 049 [[2311.00020](#)].
- [3] R. Alonso, B. Grinstein and J. Martin Camalich, *Lepton universality violation and lepton flavor conservation in B-meson decays*, *JHEP* **10** (2015) 184 [[1505.05164](#)].
- [4] B. Capdevila, A. Crivellin, S. Descotes-Genon, L. Hofer and J. Matias, *Searching for New Physics with $b \rightarrow s\tau^+\tau^-$ processes*, *Phys. Rev. Lett.* **120** (2018) 181802 [[1712.01919](#)].
- [5] J. Kumar, D. London and R. Watanabe, *Combined Explanations of the $b \rightarrow s\mu^+\mu^-$ and $b \rightarrow c\tau^-\bar{\nu}$ Anomalies: a General Model Analysis*, *Phys. Rev. D* **99** (2019) 015007 [[1806.07403](#)].
- [6] C. Cornella, J. Fuentes-Martin and G. Isidori, *Revisiting the vector leptoquark explanation of the B-physics anomalies*, *JHEP* **07** (2019) 168 [[1903.11517](#)].
- [7] C. Cornella, D. A. Faroughy, J. Fuentes-Martin, G. Isidori and M. Neubert, *Reading the footprints of the B-meson flavor anomalies*, *JHEP* **08** (2021) 050 [[2103.16558](#)].
- [8] LHCb collaboration, *Searches for $B^0 \rightarrow K^+\pi^-\tau^+\tau^-$ and $B_s^0 \rightarrow K^+K^-\tau^+\tau^-$ decays*, [2510.13716](#).
- [9] BELLE-II collaboration, *Search for $B^0 \rightarrow K^{*0}\tau^+\tau^-$ Decays at the Belle II Experiment*, *Phys. Rev. Lett.* **135** (2025) 151801 [[2504.10042](#)].
- [10] C. Bobeth and U. Haisch, *New Physics in Γ_{12}^s : $(\bar{s}b)(\bar{\tau}\tau)$ Operators*, *Acta Phys. Polon. B* **44** (2013) 127 [[1109.1826](#)].
- [11] A. Crivellin, C. Greub, D. Müller and F. Saturnino, *Importance of Loop Effects in Explaining the Accumulated Evidence for New Physics in B Decays with a Vector Leptoquark*, *Phys. Rev. Lett.* **122** (2019) 011805 [[1807.02068](#)].
- [12] M. Algueró, J. Matias, B. Capdevila and A. Crivellin, *Disentangling lepton flavor universal and lepton flavor universality violating effects in $b \rightarrow s\ell^+\ell^-$ transitions*, *Phys. Rev. D* **105** (2022) 113007 [[2205.15212](#)].
- [13] W. Altmannshofer, P. Ball, A. Bharucha, A. J. Buras, D. M. Straub and M. Wick, *Symmetries and Asymmetries of $B \rightarrow K^*\mu^+\mu^-$ Decays in the Standard Model and Beyond*, *JHEP* **01** (2009) 019 [[0811.1214](#)].
- [14] W. Detmold and S. Meinel, $\Lambda_b \rightarrow \Lambda\ell^+\ell^-$ form factors, differential branching fraction, and angular observables from lattice QCD with relativistic b quarks, *Phys. Rev. D* **93** (2016) 074501 [[1602.01399](#)].
- [15] M. Beneke, T. Feldmann and D. Seidel, *Systematic approach to exclusive $B \rightarrow Vl^+l^-$, $V\gamma$ decays*, *Nucl. Phys. B* **612** (2001) 25 [[hep-ph/0106067](#)].

- [16] H. M. Asatrian, C. Greub and J. Virto, *Exact NLO matching and analyticity in $b \rightarrow s\ell\ell$* , *JHEP* **04** (2020) 012 [1912.09099].
- [17] M. Bordone, G. Isidori, S. Mächler and A. Tinari, *Short- vs. long-distance physics in $B \rightarrow K^{(*)}\ell^+\ell^-$: a data-driven analysis*, *Eur. Phys. J. C* **84** (2024) 547 [2401.18007].
- [18] P. Böer, T. Feldmann and D. van Dyk, *Angular Analysis of the Decay $\Lambda_b \rightarrow \Lambda(\rightarrow N\pi)\ell^+\ell^-$* , *JHEP* **01** (2015) 155 [1410.2115].
- [19] T. Blake and M. Kreps, *Angular distribution of polarised Λ_b baryons decaying to $\Lambda\ell^+\ell^-$* , *JHEP* **11** (2017) 138 [1710.00746].
- [20] M. Bordone, M. Rahimi and K. K. Vos, *Lepton flavour violation in rare Λ_b decays*, *Eur. Phys. J. C* **81** (2021) 756 [2106.05192].
- [21] L. collaboration, R. Aaij, A. S. W. Abdelmotteleb, C. A. Beteta, F. Abudinén, T. Ackernley et al., *Measurement of the branching fraction of the $\Lambda_b^0 \rightarrow j\psi\lambda$ decay and isospin asymmetry of $b \rightarrow j\psi k$ decays*, 2025.
- [22] PARTICLE DATA GROUP collaboration, *Review of particle physics*, *Phys. Rev. D* **110** (2024) 030001.
- [23] M. Bordone, G. Isidori and A. Pattori, *On the Standard Model predictions for R_K and R_{K^*}* , *Eur. Phys. J. C* **76** (2016) 440 [1605.07633].
- [24] Y. Amhis, M. Bordone and M. Reboud, *Dispersive analysis of $\Lambda_b \rightarrow \Lambda(1520)$ local form factors*, *JHEP* **02** (2023) 010 [2208.08937].
- [25] D. van Dyk, M. Reboud, M. Kirk, N. Gubernari, P. Lüghausen, D. Leljak et al., *EOS version 1.0.17*, 2025. 10.5281/zenodo.3376590.
- [26] EOS AUTHORS collaboration, *EOS: a software for flavor physics phenomenology*, *Eur. Phys. J. C* **82** (2022) 569 [2111.15428].
- [27] LHCb collaboration, *Differential branching fraction and angular analysis of $\Lambda_b^0 \rightarrow \Lambda\mu^+\mu^-$ decays*, *JHEP* **06** (2015) 115 [1503.07138].
- [28] LHCb collaboration, *Measurement of the branching fraction of the $\Lambda_b^0 \rightarrow J/\psi\Lambda$ decay and isospin asymmetry of $B \rightarrow J/\psi K$ decays*, 2509.12805.
- [29] T. Blake, S. Meinel and D. van Dyk, *Bayesian Analysis of $b \rightarrow s\mu^+\mu^-$ Wilson Coefficients using the Full Angular Distribution of $\Lambda_b \rightarrow \Lambda(\rightarrow p\pi^-)\mu^+\mu^-$ Decays*, *Phys. Rev. D* **101** (2020) 035023 [1912.05811].
- [30] L. Allwicher, M. Bordone, G. Isidori, G. Piazza and A. Stanzione, *Probing third-generation New Physics with $K \rightarrow \pi\nu\bar{\nu}$ and $B \rightarrow K^{(*)}\nu\bar{\nu}$* , Jan., 2025. 10.48550/arXiv.2410.21444.

- [31] LHCb collaboration, *Comprehensive analysis of local and nonlocal amplitudes in the $B^0 \rightarrow K^{*0} \mu^+ \mu^-$ decay*, *JHEP* **09** (2024) 026 [2405.17347].
- [32] LHCb collaboration, *Amplitude Analysis of the $B^0 \rightarrow K^{*0} \mu^+ \mu^-$ Decay*, *Phys. Rev. Lett.* **132** (2024) 131801 [2312.09115].
- [33] M. Smith, *Searching for new physics at lhcb with the flavour-changing neutral-current decay $B^0 \rightarrow K^{*0} \mu^+ \mu^-$* , *CERN Seminar, September 2025* .
- [34] G. Isidori, Z. Polonsky and A. Tinari, *Explicit estimate of charm rescattering in $B^0 \rightarrow K^0 \ell^+ \ell^-$* , *Phys. Rev. D* **111** (2025) 093007 [2405.17551].
- [35] G. Isidori, Z. Polonsky and A. Tinari, *Charm rescattering in $B^0 \rightarrow K^0 \ell^+ \ell^-$: an improved analysis*, 2507.17824.
- [36] T. Feldmann and M. W. Y. Yip, *Form factors for $\Lambda_b \rightarrow \Lambda$ transitions in the soft-collinear effective theory*, *Phys. Rev. D* **85** (2012) 014035 [1111.1844].
- [37] A. Datta, S. Kamali, S. Meinel and A. Rashed, *Phenomenology of $\Lambda_b \rightarrow \Lambda_c \tau \bar{\nu}_\tau$ using lattice QCD calculations*, *JHEP* **08** (2017) 131 [1702.02243].